Antiproton and Electron Plasma Behavior and its Control for Production of Ultraslow Antiproton Beams

N. Kuroda*, H.A. Torii†, M. Shibata*, Y. Nagata†, D. Barna**, M. Hori‡, A. Mohri*, K. Komaki† and Y. Yamazaki*,†

*RIKEN, 2-1 Hirosawa, Wako-shi, Saitama, 351-0198, Japan
†Institute of Physics, University of Tokyo, 3-8-1 Komaba, Meguro-ku, Tokyo, 153-8902, Japan
**KFKI Research Institute of Particle and Nuclear Physics, H-1525 Budapest, Hungary
‡CERN, CH-1211 Genève, Switzerland

Abstract. For the production of ultraslow antiproton beams, decelerated antiprotons were captured in an electro-magnetic trap and cooled by collisions with preloaded electrons. This electron cooling feature was non-destructively monitored by measurement of electrostatic oscillations of the electron plasma. The radial distribution of the plasma was controlled for efficient cooling and extraction by utilizing rotating wall field technique.

Keywords: antiproton, non-neutral plasma, multiring trap
PACS: 39.10.+j, 52.27.Jt, 52.35.Fp

INTRODUCTION

The ASACUSA (Atomic Spectroscopy And Collisions Using Slow Antiprotons) experiment prepared an intense ultraslow antiproton source, MUSASHI (Monoenergetic Ultra-Slow Antiproton Source for High-precision Investigation) with the sequential combination of the CERN Antiproton Decelerator (AD) and the radio frequency quadrupole decelerator (RFQD). The ultraslow antiproton beam is an important step to the study of the initial processes of antiprotonic atom ($\bar{p}A^+$) formation [1] and to the synthesis and the study of antihydrogen [2]. Such exotic atoms can only be efficiently synthesized from component particles at eV and lower energies.

MUSASHI is composed of two parts, a multiring electrode trap (MRT) [3] and a transport beam line for ultraslow antiproton beams [4]. The energetic antiprotons were captured and cooled via collisions with preloaded electrons in the MRT. About 1.2×10^6 of the captured antiprotons could be stored in the MRT [5]. After the cooling, antiprotons were extracted to the field free region via the transport beam line.

Figure 1 shows a schematic view of the MRT housed in a superconducting solenoid. By applying a proper voltage on each ring electrode comprising the MRT, an electrostatic potential expressed approximately as a quadratic function along the axis was produced. This potential is called the harmonic potential. The electrons as a coolant were injected from the downstream side of the MRT. The typical number of stored electrons was around 3×10^8. They formed a nonneutral plasma in the harmonic potential well after having quickly dissipated their energy via synchrotron radiation cooling [6] under the strong magnetic field. The shape of the electron plasma is spheroid under a rigid

CP796 Low Energy Antiproton Physics-LEAP '05
edited by Dieter Grzonka, Rafał Czyżykiewicz, Walter Oelert, Tomasz Rożek, and Peter Winter

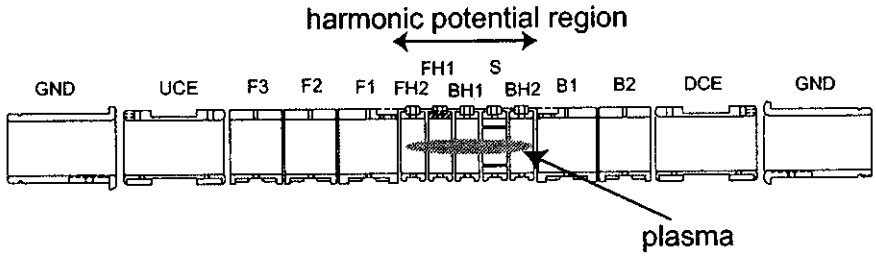

FIGURE 1. Schematic view of the MRT. The electrode "S" is segmented azimuthally.

rotor equilibrium [7].

One of the ring electrodes was azimuthally segmented into 4 sections so that a rf field could be applied to compress the plasma or charged particle cloud in the MRT.

EXPERIMENTS

Plasma temperature diagnosis

When the boundary of the plasma is assumed to be sharp even in a finite temperature, the angular frequency of electrostatic oscillation of cold spheroidal plasmas, ω_l, is given by [8, 9, 10],

$$\frac{\varepsilon_3}{\varepsilon_0} = 1 - \frac{\omega_p^2}{\omega^2}\left(1 + \frac{3k_B T_e}{m_e}\frac{k^2}{\omega^2}\right) = \left(\frac{\alpha - \varepsilon_3/\varepsilon_0}{\alpha^2 - 1}\right)^2 \frac{P_l(\xi_1)Q_l'(\xi_2)}{P_l'(\xi_1)Q_l(\xi_2)}, \tag{1}$$

where $\xi_1 = \alpha(\alpha^2 - \varepsilon_3/\varepsilon_0)^{-1/2}$, and $\xi_2 = \alpha(\alpha^2 - 1)^{1/2}$. Here ε_3 is the dielectric tensor element along the magnetic field, ε_0 is the vacuum dielectric constant, l is the node number of the oscillation along the axis, a is the radius of the spheroid, $2b$ is the length of the plasma, $\alpha = b/a$ is the aspect ratio, and k is the wave number of the electrostatic wave. P_l and Q_l represent Legendre functions of the first and second kinds, while P_l' and Q_l' denote their derivatives. Here $\omega_p = \sqrt{n_e q^2/\varepsilon_0 m_e}$ is the angular frequency of the plasma oscillation where n_e is the number density of the electrons, q is the electron's charge, m_e is the mass.

The plasma modes were monitored continuously by applying a white noise to the plasma via one of the trap electrodes. The noise excited axially symmetric electrostatic oscillation, (l,0) modes, of the plasma. These oscillations appeared as peaks in the power spectrum at the corresponding mode frequencies. Figure 2 is an example of the time evolution of the power spectrum where the resonance corresponding to the (1,0), (2,0), and (3,0) modes are clearly observed. The resonance frequency of the (1,0) mode was almost constant during and after the antiproton injection. This figure was compared with the frequencies of the (2,0) and (3,0) modes, which increased after the antiproton injection, reached a maximum in a few seconds, and then slowly returned to the initial frequencies in about 30 s. Such a frequency variation is due to heat-up of the electron plasma by the antiproton injection followed by the cooling via synchrotron radiation.

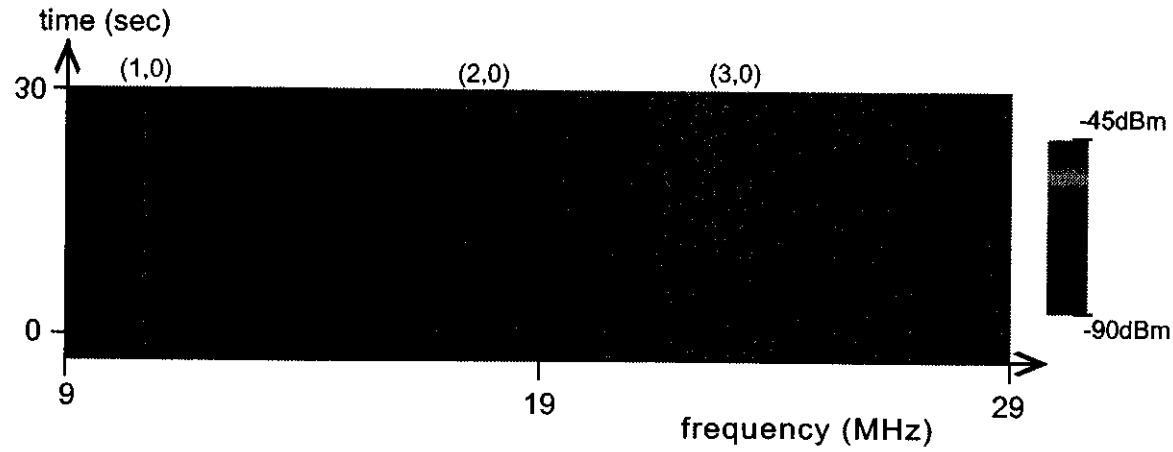

FIGURE 2. Time evolution of the power versus frequency spectrum of the electron plasma after antiproton injection at $t = 0$. The three arrowed regions correspond to the (1,0), (2,0), and (3,0) modes, respectively.

This figure was used to monitor the antiproton cooling process. On the other hand, the (1,0) mode frequency has no temperature dependence as is expected from Eq.1.

The temperature of the electron plasma was evaluated from the frequency shift by using Eq. 1. Both (2,0) and (3,0) shifts after the antiproton injection corresponded to the temperature shift, which was around 0.6 eV at the maximum.

Considering the experimentally obtained synchrotron radiation cooling time, $\tau_c[\mathrm{s}] \sim 8.6/B[\mathrm{T}]^2$, the energy transfer between the beam to the plasma is found by solving the simultaneous equation with respect to time t. This calculation reproduces the experimentally obtained time evolution of the electron plasma temperature.

Radial distribution control

A rotating rf field can apply a torque for confined plasmas, and so the radial distribution of the plasma is controlled [11, 12].

In this experiment, the radial distribution of the electron plasma was successfully controlled by rotating electric dipole field whose frequency and amplitude were around 2 MHz and 0.8 V_{pp}. Without any radial distribution control, a considerable amount of injected antiprotons which did not overlap with the electron plasma and hence were not cooled and trapped in the trapping region were lost when the catching potential of the MRT was turned off, because the initial radius of the electron plasma was smaller than the antiproton beam. To collect much more antiprotons, the counter-rotating electric dipole fields were applied. These dipole field rotated inversely against the direction of rigid rotation of the electron plasma, and so the plasma was expanded. This technique was useful to confine a lot of antiprotons and make an intense ultraslow antiproton beam.

SUMMARY

The cooling process of injected antiprotons to the MRT was non-destructively observed by monitoring electrostatic mode frequencies of the preloaded electron plasma.

The radial distribution of the electron plasma was controlled by utilizing rotating electric field technique. The broad injected antiproton beams were cooled by the electron plasma expanded by the counter-rotating electric field.

These diagnosis and control technique was utilized to produce intense ultraslow antiproton beams.

ACKNOWLEDGMENTS

This work was supported by the Grant-in-Aid for Creative Scientific Research (10P0101) of the Japanese Ministry of Education, Culture, Sports, Science and Technology (MonbuKagaku-shō), Special Research Projects for Basic Science of RIKEN, and the Hungarian National Science Foundation (OTKA T033079).

REFERENCES

1. Y. Yamazaki, *Nucl. Instrum. Methods Phys. Res. B*, **154**, 174 (1999.
2. A. Mohri, and Y. Yamazaki, *EuroPhys. Lett.* **63**, 207 (2003).
3. A. Mohri, H. Higaki, H. Tanaka, Y. Yamazawa, M. Aoyagi, T. Yuyama, and T. Michishita, *Jpn. J. Appl. Phys.* **37**, 664 (1998).
4. K. Yoshiki Franzen, N. Kuroda, H. A. Torii, M. Hori, Z. Wang, H. Higaki, S. Yoneda, B. Juhász, D. Horváth, A. Mohri, K. Komaki, and Y. Yamazaki, *Rev. Sci. Instrum.* **74**, 3305 (2003).
5. N. Kuroda, H. A. Torii, K. Yoshiki Franzen, Z. Wang, S. Yoneda, S. Inoue, M. Hori, B. Juhász, D. Horváth, H. Higaki, A. Mohri, J. Eades, K. Komaki, and Y. Yamazaki, *Phys. Rev. Lett.* **94**, 023401 (2005).
6. B. Beck, J. Fajans, and J. Malmberg, *Phys. Plasmas* **3**, 1250 (1996).
7. R. C. Davidson, *PHYSICS OF NONNEUTRAL PLASMAS*, Imperial College Press and World Scientific, London, 2001.
8. D. Dubin, *Phys. Rev. Lett.* **66**, 2076 (1991).
9. M. Tinkle, R. Greaves, C. Surko, R. Spencer, and G. Mason, *Phys. Rev. Lett.* **72**, 352 (1994).
10. H. Higaki, N. Kuroda, T. Ichioka, K. Yoshiki Franzen, Z. Wang, K. Komaki, and Y. Yamazaki, *Phys. Rev. E* **65**, 046410 (2002).
11. X.-P. Huang, F. Anderegg, E. Hollmann, C. Driscoll, and T. O'Neil, *Phys. Rev. Lett.* **78**, 875 (1997).
12. F. Anderegg, E. Hollmann, and C. Driscoll, *Phys. Rev. Lett.* **81**, 4875 (1998).